arXiv:1210.3220v1 [cond-mat.mes-hall] 11 Oct 2012

Annealing-induced magnetic moments detected by spin precession measurements in epitaxial graphene on SiC

Bastian Birkner,[1,*] Daniel Pachniowski,[1] Andreas Sandner,[1] Markus Ostler,[2] Thomas Seyller,[2,†] Jaroslav Fabian,[3] Mariusz Ciorga,[1] Dieter Weiss,[1] and Jonathan Eroms[1]

[1]*Institute of Experimental and Applied Physics, University of Regensburg, 93040 Regensburg, Germany*
[2]*Lehrstuhl für Technische Physik, University of Erlangen-Nürnberg, 91058 Erlangen, Germany*
[3]*Institute of Theoretical Physics, University of Regensburg, 93040 Regensburg, Germany*

(Dated: October 12, 2012)

We present results of non-local and three terminal (3T) spin precession measurements on spin injection devices fabricated on epitaxial graphene on SiC. The measurements were performed before and after an annealing step at 150 °C for 15 minutes in vacuum. The values of spin relaxation length L_s and spin relaxation time τ_s obtained after annealing are reduced by a factor 2 and 4, respectively, compared to those before annealing. An apparent discrepancy between spin diffusion constant D_s and charge diffusion constant D_c can be resolved by investigating the temperature dependence of the g-factor, which is consistent with a model for paramagnetic magnetic moments.

PACS numbers: 72.25.-b,72.80.Vp,85.75.-d

Apart from its prospects for electronic devices[1,2] single layer graphene (SLG) is also a very promising candidate in the field of spintronics because it is expected that spin information can be passed in graphene over long distances[3] due to the weak spin-orbit coupling and low hyperfine interaction[4]. Up to now, however, the measured spin lifetimes in exfoliated SLG (0.5 ns at RT[5], ≈ 1 ns at 4 K[6]) and also in bilayer graphene (≈ 2 ns at RT[7]) on SiO_2 are still one order of magnitude smaller than in conventional semiconductor heterostructures. Even if the mobility μ for graphene on SiO_2 is modified by e.g. ligand-bound nanoparticles[8] (2700 cm^2/Vs - 12 000 cm^2/Vs) or by using high quality suspended graphene devices[9] ($\mu > 100\,000$ cm^2/Vs), measured spin lifetimes are below 2 ns. Similar values of τ_s, slightly over 2 ns, were also reported for graphene epitaxially grown on a semi-insulating silicon carbide (SiC) substrate[10,11] using a direct non-local measurement[12] while a huge τ_s was obtained by an indirect[13] method. In Ref. 12 also a large difference between D_c and D_s was reported, which was first ascribed to spin storage in localized states and later reinterpreted using a modified g-factor[14]. McCreary *et al.*[15] studied the influence of artificially created paramagnetic moments on spin transport in graphene, and introduced an effective exchange field model leading to an enhanced g-factor. This variety of different results and ambiguity in their interpretation motivates further experiments on epitaxial graphene to understand the spin relaxation mechanism in order to control the spin information for future spintronic devices.

Here we also use epitaxial graphene grown on the Si face of SiC and present non-local and three terminal[16] spin precession measurements. The latter probes the spin accumulation[17] directly underneath the injector electrode induced electrically by a spin polarized current. We compare the results before and after an annealing step and observe that our measurements after annealing can be well explained with an enhanced g-factor assuming that charge (D_c) and spin diffusion constants (D_s) are equal. As the temperature dependence of this increased g-factor shows a clear $1/T$ (paramagnetic) behavior, we believe that annealing creates local magnetic moments via e.g. vacancies[18] which influence the spin transport properties.

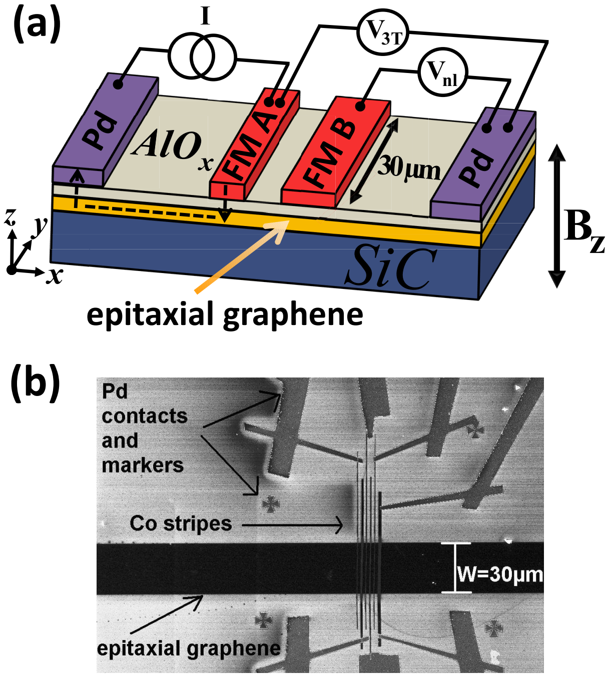

FIG. 1. (Color online) **(a)** Schematic drawing of the non-local and 3T measurement setup which is used for electrical spin injection and detection. The magnetic field B_z is applied along the z axis. **(b)** SEM picture of the epitaxial graphene spin valve device.

Fig. 1(a) shows a sketch of the applied measurement methods, Fig. 1(b) a SEM picture of the used epitaxial graphene spin valve device. The graphene stripes having

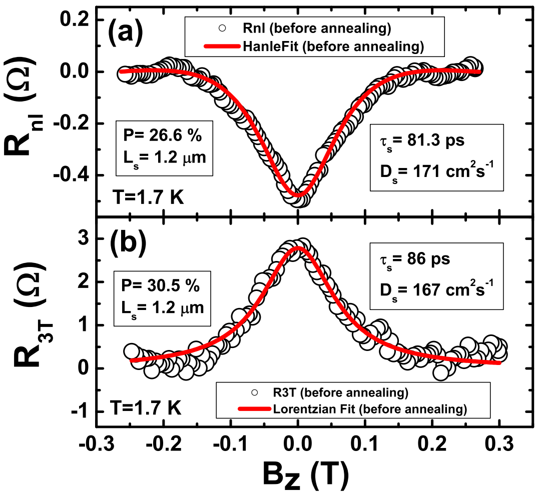

FIG. 2. (Color online) **(a)** Hanle spin precession measurement (background removed) with a DC current of +10 μA at 1.7 K and fit (continuous line) in non-local configuration. **(b)** 3T measurement (background removed) and Lorentzian fit (continuous line). Both measurements are done *before* an annealing step.

a width of $W = 30$ μm and a length of about 750 μm are produced using a negative resist based electron beam lithography (EBL) step and oxygen plasma etching for 30 s (30 mTorr O_2, 50 W). Afterwards a thin tunneling barrier (AlO_x) with a thickness of about 1 nm was produced by depositing Al atoms over the entire cooled sample (180 K) in a UHV system ($p \approx 10^{-9}$ mbar) and subsequent oxidation in the load lock in pure oxygen atmosphere ($p \approx 3 \times 10^{-2}$ mbar) at RT for 30 minutes. This AlO_x tunneling barrier with a contact resistance $R_c \geq 2$ $k\Omega$ provides high spin injection efficiencies and reduces spin relaxation induced by the contacts[19]. The ferromagnetic (FM) cobalt electrodes (Co 20 nm) with a width of 200 nm (contact A) and 500 nm (contact B) and the non-magnetic palladium contacts (Pd 80 nm) were each patterned using a positive PMMA resist based EBL step. The evaporation is done via electron gun (Co) and thermally (Pd) at a base pressure of about 5×10^{-7} mbar followed by a standard lift-off technique. The distance L between the edges of the FM stripes is 2 μm. Finally the sample is glued into a chip carrier and the measurements are done using a standard DC setup in a Cryogenics He-4 cryostat ($T = 1.6 \ldots 300$ K) equipped with a vector magnet ($B_{x,y,z} = -1 \ldots 1$ T). The complete sample fabrication is done without applying a high temperature cleaning step.

In Fig. 2 typical Hanle curves in the non-local and three terminal setup at 1.7 K are shown when using contact A as an injector. The FM stripes are magnetized in parallel configuration and the magnetic field B_z is applied out-of plane which leads to dephasing of the spin signal. The continuous curve for the non-local curve in Fig. 2(a) is the numerical fit with the solution of the following equation[20]

$$R_{nl} = \frac{V_{nl}}{I} = \frac{P^2 R_s L_s}{2W} \int_0^\infty \frac{cos(\omega_L t)}{\sqrt{4\pi D_s t}} e^{\frac{-(x_2 - x_1 - v_d t)^2}{4 D_s t}} e^{\frac{-t}{\tau_s}} dt \tag{1}$$

where P is assumed to be the same for both FM stripes and x_1, x_2 are the points of injection and detection, respectively. P is the spin injection efficiency, I the injection current, $\omega_L = g\mu_B B_z/\hbar$ the Larmor frequency with the Landé factor g, R_s is the sheet resistance of graphene, W the width of the graphene stripe, D_s is the spin diffusion constant, finally τ_s and $L_s = \sqrt{D_s \tau_s}$ are the spin relaxation time and length, respectively. The Hanle signal R_{3T} in 3T configuration (Fig. 2(b)) decays with B_z due to spin dephasing with a Lorentzian shape[16] according to:

$$R_{3T} = \frac{V_{3T}}{I} = \frac{P^2 R_s L_s}{2W(1 + (\omega_L \cdot \tau_s)^2)} \tag{2}$$

As the amplitude of the non-local signal is determined by the product of P^2 and L_s these parameters are not independent in the fitting procedure. Therefore $L_s = 1.2$ μm is estimated assuming an exponential decay of the spin signal given by $R_{3T}(B_z = 0)$ at $L = 0$ μm and $R_{nl}(B_z = 0)$ at $L = 2$ μm. Now P and τ_s are the free fitting parameters and D_s can be calculated via $D_s = L_s^2/\tau_s$.

In Fig. 2 one can see that for both non-local and 3T spin precession measurements the results for P, τ_s and D_s are almost identical. This agreement indicates that these signals originate from an induced spin accumulation into graphene. Slight differences especially in the spin injection efficiency P can be explained by a small anisotropic magneto resistance contribution of about 0.5 Ω of the FM stripes to R_{3T} determined in reference measurements (not shown). This small deviation leads to an absolute error of L_s of about $\Delta L_s = 200$ nm. The spin diffusion constant $D_s = 171$ cm^2/s has the same order of magnitude as the charge diffusion constant $D_c = 120$ cm^2/s extracted from another epitaxial graphene sample grown with identical parameters. This reference sample was measured in van der Pauw geometry to determine the sheet resistance $R_s = 4.15$ kΩ. From low field Hall measurements we get the charge carrier density $n = 5.25 \times 10^{11}$ cm^{-2} and the mobility $\mu = 1/(R_s n e) = 2870$ cm^2/Vs. The reference sample also showed the quantum Hall effect starting at approximately 4 T, underlining the high sample quality. Due to a different sample preparation (AlOx on top of graphene) for our spin valve device ($R_s = 1.5$ kΩ) D_c can differ from the reference sample and we therefore take D_c to be identical to D_s as determined from the Hanle spin signals. By fitting the non-local and 3T measurements, we obtain $\tau_s = 80$ ps which is slightly smaller than in exfoliated SLG[3,19,21].

In order to check if annealing influences the charge transport properties and/or the induced spin accumula-

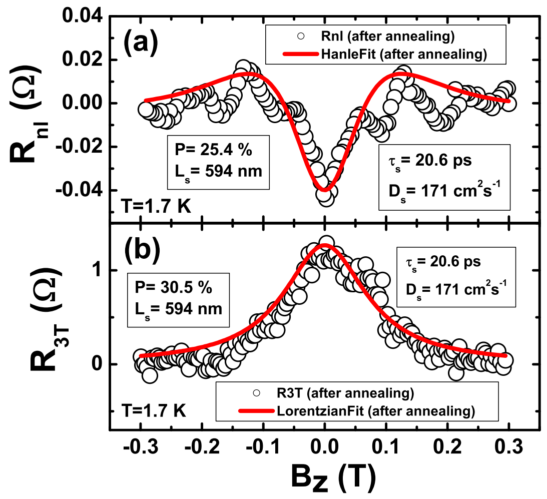

FIG. 3. (Color online) **(a)** Hanle spin precession measurement (background removed) at 1.7 K and fit (continuous line) in non-local configuration. **(b)** 3T measurement (background removed) and Lorentzian fit (continuous line). Both measurements are done *after* an annealing step. The fittings are done treating the g-factor as a free parameter.

tion, a post annealing step is done at 150 °C for 15 minutes in vacuum to avoid intercalation of hydrogen[22,23] via forming gas. Then we repeat the same spin precession measurements as before and interestingly we observe that τ_s increases whereas D_s is decreased by almost a factor of 5 if we assume the same g-factor as before annealing ($g = g_0 = 2$). For the configuration with contact B as an injector we observe an even bigger decrease of D_s by a factor of about 10 (Table I). At this point we conclude that annealing affects the spin transport properties and we observe the same apparent reduction of D_s as in Ref. 12, where a high temperature annealing step was included in the sample preparation procedure. The fact that both L_s and the 3T amplitude (1.3 Ω) at zero magnetic field decrease by almost the same factor indicates that the applied post annealing step also affects the induced spin accumulation underneath the injector electrode. A slightly higher sheet resistance ($R_s = 1.7$ kΩ) indicates that the charge transport properties are only weakly influenced after annealing, that means we have the following situation: $D_c^{before} \approx D_c^{after} \gg D_s^{after}$. $L_s = 594$ nm is reduced by a factor of 2 after annealing and is again extracted from the exponential decay of the spin signal at the injection point ($R_{3T}(0)$) and at a distance $L = 2$ μm ($R_{nl}(0)$).

In an attempt to understand the discrepancy of D_c and D_s Maassen *et al.*[12] first considered localized states in the electrically inert buffer layer[24] (BL) which could provide hopping sites for the spins being able to change the spin transport properties but not the charge transport properties. The difference in D_s and D_c was also recently discussed by McCreary *et al.*[15]. They assume a formation of local magnetic moments by Ar sputtering or from hydrogen adatoms on exfoliated graphene samples which provide an enhanced magnetic field for the diffusing spins, which can be modeled by an effective g-factor. Maassen *et al.*[14] reinterpreted their experiments[12] using a model of localized states, where the effective Larmor frequency is increased in the limit of strong coupling, which again can be expressed by an enhanced g-factor.

Before annealing				After annealing					
τ_s	D_s	g_0	**Injector**	τ_s	D_s	g_0	τ_s	D_s	g_{eff}
81.3	171	2	A	95	37	2	20.6	171	6.5
108	208	2	B	197	20	2	23.0	171	8.7

TABLE I. D_s [cm^2/s], τ_s [ps] and g-factor before and after annealing for injector contact A and B. After annealing the measurements can also be fitted with an enhanced $g_{eff} > g_0$.

For this reason we also fit our non-local and 3T data after annealing, treating the g-factor in the Larmor frequency (Eqs. (1) and (2)) as a free parameter, and assuming $D_c^{after} = D_s^{after} = 171$ cm^2/s. Fig. 3 shows that our data can also be well fitted with an enhanced g-factor of 6.5 in the non-local and 6.7 in the 3T setup, respectively. The oscillations observed in the Hanle curve (Fig. 3(a)) at higher magnetic fields are phase coherent contributions and vanish at higher temperatures. If we summarize our experimental findings so far (Table I) we can conclude that our measurements after annealing can be explained either by $D_c^{after} \neq D_s^{after}$ or by an effective Landé factor $g_{eff} > 2$ as both models reproduce the data equally well since Eqs. (1) and (2) contain the g-factor implicitly in the Larmor frequency ω_L and are invariant under a rescaling of g, τ_s and D_s.

To determine which model (hopping or magnetic moments) is appropriate in our situation we study the temperature dependence of spin transport. We observe that the enhanced effective g-factor, as well as the amplitude of the spin signal, decrease with increasing temperature (Fig. 4). If g_{eff} originates from magnetic moments then its temperature dependence can be described by the following equation[15]:

$$g_{eff}(T) = g_0 + \frac{g_0 \eta_M A_{ex}}{k_B T} \tag{3}$$

This is the low field approximation of the Brillouin function of a spin 1/2 paramagnetic material. A_{ex} is the strength of the exchange coupling, η_M represents the filling density of the magnetic moments, $g_0 = 2$ is the g-factor for free electrons and k_B is the Boltzmann constant. As it is seen in Fig. 5 the measured temperature dependence of g_{eff} is well described by Eq. (3). This temperature dependence is compatible with the effective exchange field model proposed by McCreary *et al.*[15] which describes the enhancement of the magnetic field felt by the diffusing spins due to localized paramagnetic moments. Maassen *et al.*[14], on the other hand, interpret

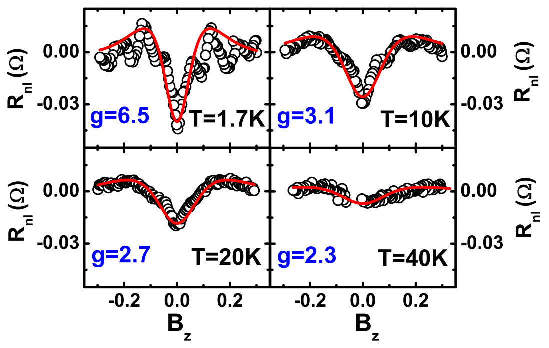

FIG. 4. (Color online) Temperature dependent non-local Hanle measurements (background removed) with g-factor as further fitting parameter.

their data by hopping of the diffusing spins into localized states, whereby they experience a dramatically higher g-factor. In their work the enhancement of g is most pronounced at room temperature, whereas in our case the maximum g_{eff} is obtained at low temperature. We therefore believe that post annealing creates an amount of randomly positioned magnetic moments resulting in an increased effective magnetic field $B_{eff} = B_z + B_{ex}$ composed of the applied out-of plane magnetic field B_z and of an exchange field B_{ex} coming from the induced magnetic moments. This enhanced magnetic field can be modeled by an effective g-factor in the Larmor frequency ω_L. As we nearly get the same Landé factor from the non-local Hanle fit and the Lorentzian fit we can not decide if the magnetic moments are formed in the graphene/buffer layer transition or at the AlO$_x$/graphene interface. The difference between our experiment and the work of Maassen *et al.*[12] may be due to different annealing conditions.

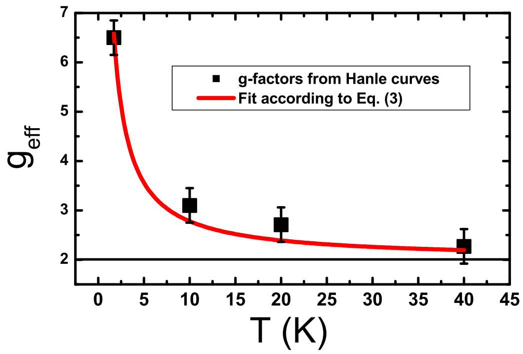

FIG. 5. (Color online) Temperature dependence of the g-factor. The continuous curve is the fit according to Eq. (3).

In conclusion, an electrically induced spin imbalance from ferromagnetic Co stripes can be analyzed via spin precession measurements in both non-local and three terminal configuration. By introducing a post annealing step, we observe that the spin relaxation length as well as the non-local and 3T Hanle amplitude decrease. Fitting of the non-local and 3T data after annealing show an increase of the g-factor if spin and charge diffusion constants are assumed to be the same. The origin of the g-factor enhancement are local magnetic moments formed by annealing. The reduced spin lifetime and length support this assumption because local magnetic moments act as an additional spin scattering source. Finally, the temperature dependence shows a clear evidence that paramagnetic moments are created as the effective g-factor scales with $1/T$ with increasing temperature.

Support from the DFG within SFB 689 “Spin phenomena in reduced dimensions” and SPP 1459 “Graphene” is gratefully acknowledged. We would like to thank F. Fromm, T. Maassen, and R. Kawakami for helpful discussions.

---

[*] bastian.birkner@physik.uni-regensburg.de
[†] Present address: Technische Universität Chemnitz, 09107 Chemnitz, Germany

[1] A. H. Castro Neto, F. Guinea, N.M.R. Peres, K.S. Novoselov, and A. K. Geim, Rev. Mod. Phys. **81**, 109 (2009).
[2] K. S. Novoselov, A. K. Geim, S. V. Morozov, D. Jiang, M. I. Katsnelson, I. V. Grigorieva, S. V. Dubonos, and A. A. Firsov, Nature (London) **438**, 197 (2005).
[3] N. Tombros, C. Józsa, M. Popinciuc, H. T. Jonkman, and Bart J. van Wees, Nature (London) **448**, 571 (2007).
[4] D. Huertas-Hernando, F. Guinea, and A. Brataas, Phys. Rev. B **74**, 155426 (2006).
[5] W. Han, K. Pi, K. M. McCreary, Y. Li, J. J. I. Wong, A. G. Swartz, and R. K. Kawakami, Phys. Rev. Lett. **105**, 167202 (2010).
[6] W. Han, and R. K. Kawakami, Phys. Rev. Lett. **107**, 047207 (2011).
[7] T.-Y. Yang, J. Balakrishnan, F. Volmer, A. Avsar, M. Jaiswal, J. Samm, S.R. Ali, A. Pachoud, M. Zeng, M. Popinciuc, G. Güntherodt, B. Beschoten, and B. Özyilmaz, Phys. Rev. Lett. **107**, 047206 (2011).
[8] W. Han, J.-R. Chen, D. Wang, K. M. McCreary, H. Wen, A. G. Swartz, J. Shi, and R. Kawakami, Nano Lett. **12**, 3443 (2012).
[9] M. H. D. Guimarães, A. Veligura, P. J. Zomer, T. Maassen, I. J. Vera-Marun, N. Tombros, and B. J. van Wees, Nano Lett. **12**, 3512 (2012).
[10] P. N. First, P. N., W. A. de Heer, T. Seyller, C. Berger, J. A. Stroscio, J.-S. Moon, MRS Bull. **35**, 296 (2010).
[11] K. V. Emtsev, A. Bostwick, K. Horn, J. Jobst, G. L. Kellogg, L. Ley, J. L. McChesney, T. Ohta, S. A. Reshanov, J. Röhrl, E. Rotenberg, A. K. Schmid, D. Waldmann, H. B. Weber, and T. Seyller, Nat. Mat. **8**, 203 (2009).

[12] T. Maassen, J. J. van den Berg, N. IJbema, F. Fromm, T. Seyller, R. Yakimova, and B. J. van Wees, Nano Lett. **12**, 1498 (2012).

[13] B. Dlubak, M.-B Martin, C. Deranlot, B. Servet, S. Xavier, R. Mattana, M. Sprinkle, C. Berger, W. A. De Heer, F. Petroff, A. Anane, P. Seneor, and A. Fert, Nature Physics **8**, 557 (2012).

[14] T. Maassen, J. J. van den Berg, E. H. Huisman, H. Dijkstra, F. Fromm, T. Seyller and B. J. van Wees, arXiv:1208.3129v1 (2012).

[15] K. M. McCreary, A. G. Swartz, W. Han, J. Fabian and R. K. Kawakami, arXiv:1206.2628v2 (2012).

[16] S. P. Dash, S. Sharma, R. S. Patel, M. P. de Jong, and R. Jansen, Nature **462**, 491 (2009).

[17] J. Fabian, A. Matos-Abiague, C. Ertler, P. Stano, and I. Zutic, Acta Phys. Slov. **57**, 565 (2007).

[18] O. V. Yazyev, and L. Helm, Phys. Rev. B **75**, 125408 (2007).

[19] M. Popinciuc, C. Józsa, P. J. Zomer, N. Tombros, A. Veligura, H. T. Jonkman, and B. J. van Wees, Phys. Rev. B **80**, 214427 (2009).

[20] M. Ciorga, A. Einwanger, U. Wurstbauer, D. Schuh, W. Wegscheider, and D. Weiss, Phys. Rev. B **79**, 165321 (2009).

[21] W. Han, and R. K. Kawakami, Phys. Rev. Lett. **107**, 047207 (2011).

[22] C. Riedl, C. Coletti, T. Iwasaki, A. A. Zakharov, and U. Starke, Phys. Rev. Lett. **103**, 246804 (2009).

[23] F. Speck, J. Jobst, F. Fromm, M. Ostler, D. Waldmann, M. Hundhausen, H. B. Weber, T. Seyller, Appl. Phys. Lett. **99**, 122106 (2011).

[24] K. V. Emtsev, F. Speck, T. Seyller, L. Ley and J. D. Riley, Phys. Rev. B **77**, 155303 (2008).